1

Fundamentals of Battery Materials and the Evolution of Advanced Characterization Techniques

1.1 Global Energy Transition

1.1.1 Core Demand for Energy Transformation

Guided by the china's dual-carbon goals of "carbon neutrality by 2050 and net-zero emissions by 2060," the proportion of renewable energy sources such as wind energy, solar energy, and tidal energy in the global energy market has been continuously increasing [1]. Promoting the transformation of the energy system from "fossil energy-dominated" to "renewable energy-centered" has long become a universal consensus of all mankind. However, new renewable energy sources generally have inherent defects of "intermittency, volatility, and regionality," which greatly restrict the progress of energy transformation. For instance, the power generation intensity of solar energy fluctuates by up to 80% during the day, while the output of wind energy drops by more than 50% at night. Therefore, developing supporting high-efficiency energy storage technologies to achieve the dynamic balance of "development-storage-utilization" of new energy will become a key driving force for the implementation of new energy reform. According to the prediction of the International Energy Agency, the global energy storage demand will exceed 15 TWh by 2030. Among various energy storage technologies, battery energy storage has become the core solution for grid peak regulation and distributed energy storage scenarios, owing to its millisecond-level fast response speed and high energy density exceeding 100 Wh/kg [2].

1.1.2 Performance Driven by Terminal Application Scenarios

In terminal application fields, popular sectors such as electric vehicles (EVs), portable consumer electronics (including smartphones, drones, etc.), and large-scale energy storage are imposing increasingly higher requirements on the technological advancement of battery energy storage [3, 4]. For example, in the transportation field, electric vehicles are developing toward the goals of "ultra-fast charging (charging to 80% capacity in 10 minutes), long driving range (exceeding 1000 km), and high safety (no thermal runaway)," while also requiring the battery energy density to increase from the current 300 Wh/kg to more than 500 Wh/kg. For 3C

consumer electronics, the pursuit of "slimmer and lighter design, long standby time (exceeding 72 hours), and fast charging (full charge in 30 minutes)" demands the battery's volumetric energy density to exceed 700 Wh/L. In the energy storage field, large-scale energy storage power stations require batteries to have a cycle life of over 10,000 cycles and a cost lower than 0.5 yuan/Wh. In addition, a few special fields such as polar scientific research and high-altitude power grids have put forward more stringent requirements, i.e., batteries must maintain a capacity retention rate of over 70% at −40 °C. These high standards and requirements for the performance of energy storage batteries in diverse application scenarios are driving battery technology to continuously make breakthroughs toward more diverse systems and better performance.

1.1.3 Industrialization and Scientific Research Pattern of Battery Technology

At present, the global battery industry has formed a development pattern of "lithium-ion batteries as the dominant type, with multiple new battery systems under parallel R&D" [5, 6]. In recent years, the global annual production capacity of lithium-ion batteries has exceeded 2 TWh, accounting for more than 85% of the energy storage market share, and has become the most mature commercialized energy storage technology. Meanwhile, other new battery systems are also continuously achieving technological breakthroughs and accelerating their commercialization process. For example, sodium-ion batteries have entered the pilot-scale production stage, and mass production of 1 GWh level is expected to be realized by 2025; all-solid-state batteries have achieved breakthrough results at the laboratory level and are gradually transitioning to the pilot-scale stage, with enterprises such as Toyota and QuantumScape planning to commercialize solid-state batteries by 2030. In the global scientific research field, the annual number of published Science Citation Index Expanded papers related to batteries has exceeded 80,000 in recent years, and the annual growth rate of patent applications has reached 15%, indicating an extremely high enthusiasm for R&D in the industry. However, it should be noted that there is a significant gap between the laboratory performance of many battery technologies and their actual industrial applications. For example, the cycle life of silicon-based anodes can exceed 1000 cycles under laboratory conditions, but after industrialization, their cycle life is far less than half of the laboratory level. The core reason lies in the insufficient in-depth understanding of the dynamic failure mechanisms of materials under actual working conditions. Therefore, it is urgent to use advanced characterization technologies to build a bridge between "scientific research achievements and industrial applications" and promote the rapid implementation of technologies.

The diagram depicted in Figure 1.1 includes the dominant position of lithium-ion batteries and R&D progress of new battery technologies. It illustrates the global battery industry pattern: lithium-ion batteries (annual capacity over 2 TWh, >85% market share) dominate, while sodium-ion and all-solid-state batteries advance toward commercialization, reflecting industry-science synergy.

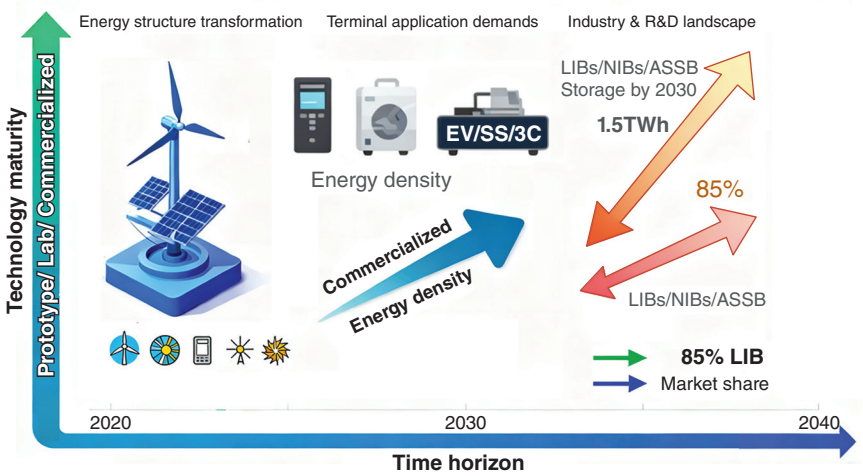


Figure 1.1 Schematic diagram of the global battery technology industry and scientific research pattern.

1.2 Basic Principles and Core Composition of Lithium-Ion Batteries

1.2.1 Working Principle of Lithium-Ion Batteries

In essence, lithium-ion batteries realize the storage and release of electrical energy through the reversible intercalation, deintercalation, and migration of lithium ions between the cathode and anodes. Precisely due to this "back-and-forth shuttling" characteristic of lithium ions, they are vividly called "rocking chair batteries" [7]. In Figure 1.2, a schematic diagram of the "rocking chair"-type working principle of lithium-ion batteries is shown. Taking $LiCoO_2$ as the cathode and graphite as the anode for specific illustration, its core electrochemical process is as follows: during charging, driven by an external electric field, the active material of the cathode undergoes an oxidation reaction, and lithium ions are deintercalated from the lattice of the cathode, then migrate to the anode through the electrolyte and separator. At the same time, the anode undergoes a reduction reaction, where lithium ions are intercalated between the layers of graphite to form the intercalation compound LiC_6, and electrons flow from the cathode to the anode through the external circuit.

Cathode oxidation reaction: $LiCoO_2 \rightarrow Li_{1-x}CoO_2 + xLi^+ + xe^-$
Anode reduction reaction: $xLi^+ + xe^- + 6C \rightarrow LiC_6$

The discharge process is completely opposite to charging. Lithium ions are deintercalated from the interlayers of graphite in the anode, migrate back to the cathode through the electrolyte, and re-intercalate into the lattice. Electrons also flow to the cathode through the external circuit, thereby realizing the discharge to external electrical devices. In the entire charge-discharge cycle system, the structure of the active materials in the cathode and anodes must have good reversibility

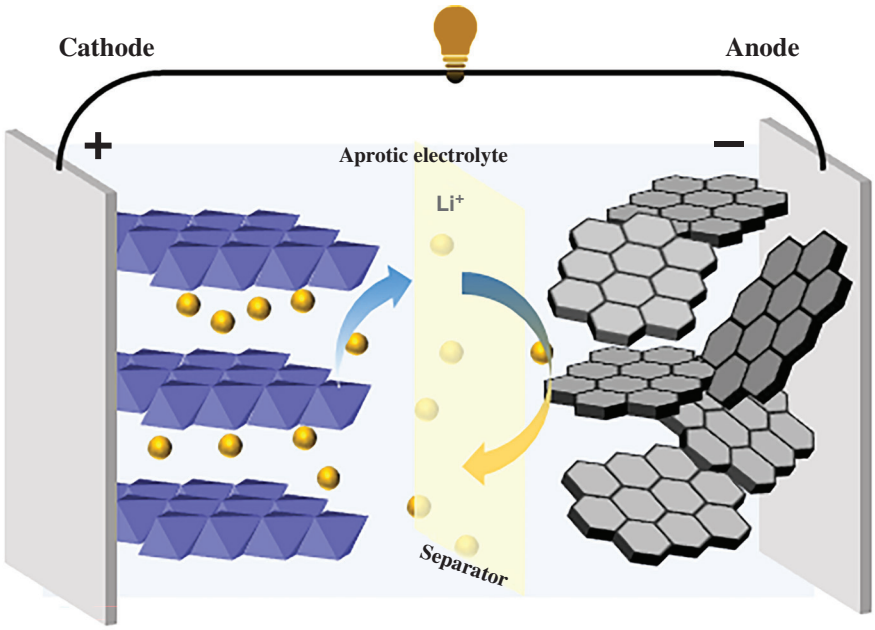


Figure 1.2 Schematic diagram of the "rocking chair"-type working principle of lithium-ion batteries.

to ensure the cycle stability of the battery; the electrolyte needs to have a high ionic conductivity of no less than 10^{-2} S/cm to ensure the rapid response of lithium ions during charge and discharge; the separator must block the passage of electrons while allowing the smooth migration of lithium ions. These components work together to ensure the efficient and stable cyclic operation of the battery.

1.2.2 Core Composition of Lithium-Ion Batteries

Figure 1.3 indicates a schematic diagram of the functional positioning of the four core components of lithium-Ion batteries (marking the core functions of the cathode, anode, electrolyte, and separator respectively) [7]. It defines each component's role: cathode (energy density determinant), anode (Li^+ storage), electrolyte (Li^+ transport), separator (electron barrier), highlighting their synergistic support for battery stability.

1. Cathode
   The cathode of a battery is mainly composed of active material, conductive agent, binder, and aluminum foil current collector. Among them, the active material accounts for 80–90% of the total mass of the cathode and is the core component that directly determines the operating voltage and capacity of the battery. At present, mainstream cathode materials are mainly divided into three categories: Layered oxides: Common types include $LiCoO_2$ and $LiNi_xCo_\gamma Mn_{1-x-\gamma}O_2$ (abbreviated as NCM). $LiCoO_2$ has an operating voltage of 3.9 V

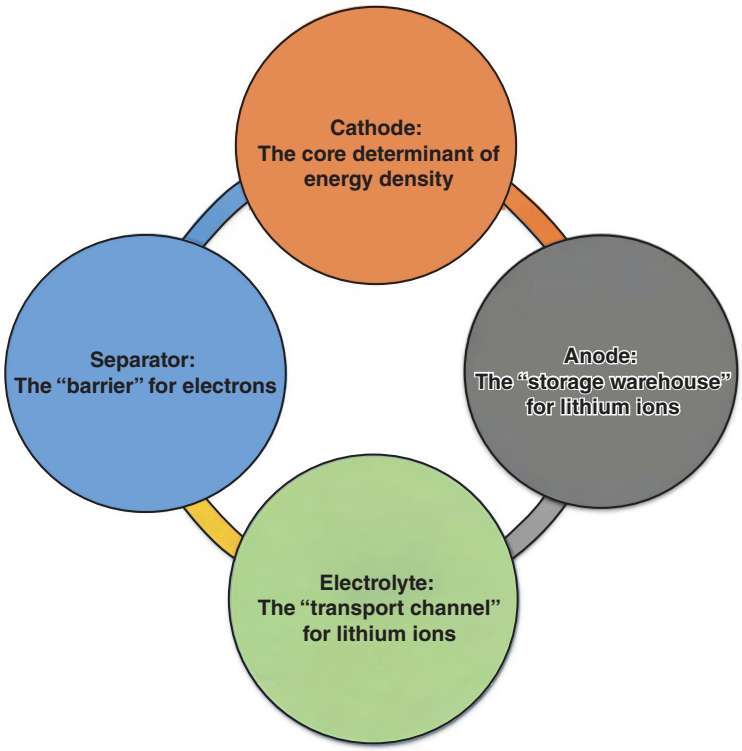


Figure 1.3 Schematic diagram of the functional positioning of the four core components of lithium-Ion batteries.

and a theoretical capacity of up to 274 mAh/g. For the NCM series, the higher the Ni content, the higher the capacity—for example, the actual capacity of NCM811 can reach 200 mAh/g. The core advantage of this type of material is its high energy density, but it is prone to oxygen release and phase transition under high-voltage conditions, which affects cycle stability. Polyanionic materials: A typical representative is $LiFePO_4$, which has an operating voltage of 3.4 V and a theoretical capacity of 170 mAh/g. Its greatest advantages are stable crystal structure and low preparation cost, making it suitable for scenarios sensitive to safety and cost, but its obvious shortcoming is relatively low energy density. Spinel-type materials: An example is $LiMn_2O_4$, which has an operating voltage of 4.1 V and a theoretical capacity of 148 mAh/g. Benefiting from its unique three-dimensional ion channel structure, it exhibits excellent rate performance, but Mn dissolution occurs under high-temperature conditions, which directly leads to rapid capacity fading of the battery.

2. Anode
The anode of a battery is composed of active material, conductive agent, binder, and copper foil current collector. Its core function is to realize the reversible storage of lithium ions, which is the key to the repeated charge and discharge

of the battery. Currently, mainstream anode materials are mainly divided into three categories: Carbon-based materials: Common types include natural graphite and hard carbon. Natural graphite has a theoretical capacity of 372 mAh/g and an interlayer spacing of 0.335 nm, and lithium ions realize lithium storage by intercalating between layers to form LiC_6. Hard carbon has a disordered structure and is more suitable for sodium-ion batteries, with a sodium storage capacity of 300–350 mAh/g. The common advantages of this type of carbon-based material are good cycle stability and low preparation cost, and they are widely used in commercial batteries. Alloy-type materials: Examples include silicon and tin. Silicon has an extremely high theoretical capacity of 4200 mAh/g and achieves high-capacity lithium storage by forming Li-Si alloys with lithium. Tin also has a theoretical capacity of 994 mAh/g. Their core advantage is that their capacity is much higher than that of carbon-based materials, but they undergo significant volume expansion during lithium intercalation—silicon, for instance, has a volume expansion rate of up to 300%, which easily leads to material pulverization and interface failure. Metallic lithium: It has a theoretical capacity of 3860 mAh/g and high energy density potential, making it an ideal anode choice for all-solid-state batteries. However, in traditional liquid electrolytes, lithium dendrites tend to grow on the surface of metallic lithium, and these dendrites may penetrate the electrolyte to cause battery short circuits, posing serious safety hazards.

3. Electrolyte

The electrolyte is the transport medium for lithium ions inside the battery. To ensure the normal operation of the battery, it must meet three core requirements: "high ionic conductivity, wide electrochemical window, and high chemical stability." Its composition usually includes lithium salt, organic solvent, and various functional additives. Lithium salt: The currently mainstream lithium salt is $LiPF_6$ with a concentration of 1 mol/L. It has a high ionic dissociation degree and can provide sufficient lithium ions for the electrolyte, but its disadvantage is that it is prone to hydrolysis to generate hydrogen fluoride (HF), which corrodes electrode materials. Auxiliary lithium salts such as LiFSI ($LiN(SO_2F)_2$) have good hydrolysis resistance and high-temperature stability, and are often used in high-voltage battery systems to improve reliability. Organic solvent: Mainly carbonate-based, including ethylene carbonate (EC), dimethyl carbonate (DMC), and ethyl methyl carbonate (EMC). EC has a high dielectric constant and can effectively promote lithium salt dissociation; DMC has low viscosity and can improve the migration rate of lithium ions; EMC can balance dielectric constant and viscosity. These three solvents are usually mixed in a volume ratio of 1:1:1 to balance dissociation efficiency and ion transport speed. Additives: Although the addition amount is only 1–5%, they play a crucial role. For example, vinylene carbonate (VC) can help form a stable solid electrolyte interphase (SEI) layer on the electrode surface; $LiPO_2F_2$ can improve the stability of the battery under high voltage; and phosphate-based additives, as flame retardants, can significantly reduce the risk of electrolyte combustion and explosion.

4. Separator
   The separator is a porous insulating material in the battery. Its core functions are, on the one hand, to physically separate the cathode and anode to prevent electronic short circuits caused by direct contact between them, and on the other hand, to allow the smooth passage of lithium ions to complete the charge-discharge cycle. Therefore, it needs to meet the key characteristics of "high porosity (30–50%), high mechanical strength, and resistance to electrolyte corrosion." Currently, mainstream separators are mainly divided into three categories: Polyolefin separators: Common types include polypropylene (PP) membranes, polyethylene (PE) membranes, or PP/PE/PP composite membranes. Their advantages are low production cost and good air permeability, and they are widely used in commercial batteries. However, their disadvantage is poor high-temperature stability and easy shrinkage—PE has a melting point of 135 °C and PP has a melting point of 165 °C, and the shrinkage risk increases significantly when the temperature exceeds the corresponding melting point. Ceramic-coated separators: They are made by coating ceramic particles such as Al_2O_3 and SiO_2 on the surface of polyolefin base membranes. They can greatly improve high-temperature anti-shrinkage performance, with a shrinkage rate of less than 5% at 150 °C, making them particularly suitable for battery products with high safety requirements. Solid electrolyte separators: Examples include lithium lanthanum zirconium oxide ceramic sheets and lithium germanium phosphorus sulfide sheets. They have both the ion-conducting function of electrolytes and the isolation function of separators, and are indispensable core components in all-solid-state batteries.

1.3 Development Trend and Core Characteristics of Secondary Batteries

1.3.1 Lithium-Ion Batteries

Since lithium-ion batteries were commercialized by Sony in 1991, as shown in Figure 1.4, they have developed a mature technical route of "layered oxide or polyanionic cathode + carbon-based or alloy-type anode + liquid electrolyte" and are widely used in various electronic devices and new energy vehicles. At present, the industry's R&D mainly focuses on three core directions: High energy density improvement: The core combination is "high-nickel ternary cathode (e.g., NCM811, NCM955) + silicon-based anode." By gradually increasing the Ni content in the cathode from 60% to 95%, the actual capacity of the cathode is increased from 160 mAh/g to approximately 220 mAh/g. For the silicon-based anode, nanostructuring (e.g., preparing Si nanoparticles) or compounding with carbon materials (e.g., constructing Si/C core-shell structures) is used to alleviate the volume expansion of up to 300% during lithium intercalation. High safety optimization: The focus is on developing cobalt-free cathodes (e.g., $LiFePO_4$/C composite cathodes, $LiNi_{0.9}Mn_{0.1}O_2$), flame-retardant electrolytes (added with

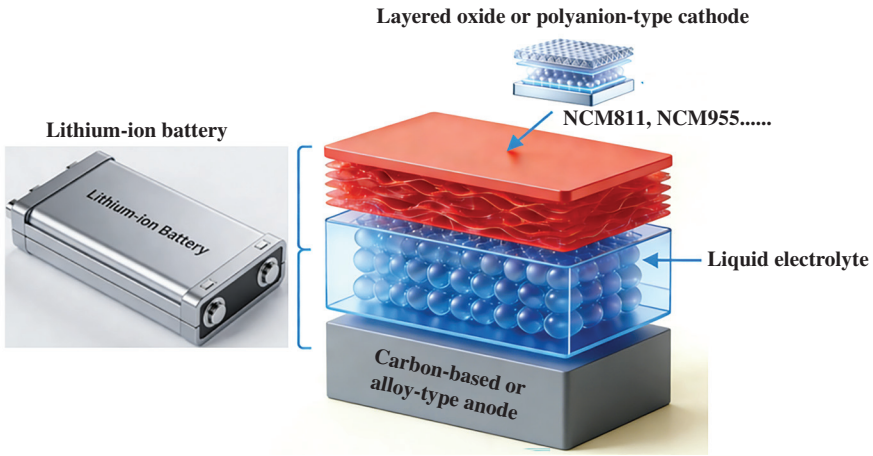


Figure 1.4 Schematic diagram of lithium-ion battery.

phosphate or fluorinated solvents), and separators with ceramic coatings on the surface, so as to reduce the risk of battery thermal runaway. Fast charging performance breakthrough: Single-crystal high-nickel cathodes are developed to reduce grain boundary impedance, and graphite/hard carbon composite anodes are designed to improve the migration rate of lithium ions, ultimately achieving a 10C fast charging effect (i.e., charging the battery to 80% capacity in 10 minutes). However, the lithium-ion battery system still faces many bottlenecks at present. For example, high-nickel cathodes are prone to lattice oxygen release during deep deintercalation, silicon-based anodes have interface failure problems, and electrolytes are prone to oxidative decomposition under high-voltage scenarios. All these factors restrict the further performance upgrade of lithium-ion batteries.

1.3.2 Sodium-Ion Batteries

Sodium-ion batteries have become a core candidate technology for large-scale energy storage scenarios due to their significant advantages: the abundance of sodium in the Earth's crust is as high as 2.36%, while that of lithium is only 0.002%, showing a prominent resource advantage; at the same time, the price of sodium salts is only 1/20 of that of lithium salts, with a distinct cost advantage; and they can maintain a capacity retention rate of over 80% at −20 °C, whose low-temperature adaptability is far superior to that of many battery systems. At present, the technical characteristics of sodium-ion batteries have gradually become clear, as shown in Figure 1.5: Cathode materials: Layered oxides (e.g., $NaNi_{0.3}Co_{0.3}Mn_{0.4}O_2$, with an actual capacity of 150–180 mAh/g) and polyanionic materials (e.g., $Na_3V_2(PO_4)_3$, with a cycle life of over 10,000 cycles) are the current mainstream choices. However, they generally face the problem of low Na^+ diffusion rate (the diffusion coefficient is only 10^{-11} cm^2/s), which restricts rate performance. Anode materials: Mainly hard carbon, which achieves a sodium storage capacity of 300–350 mAh/g through the dual mechanism

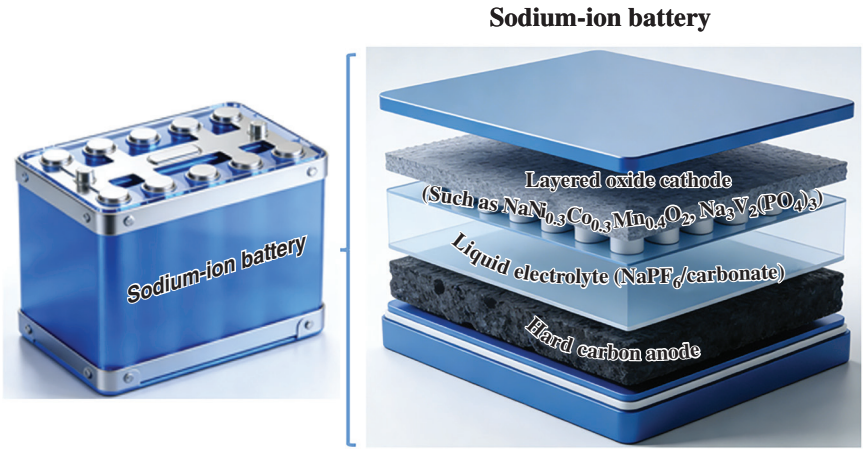


Figure 1.5 Schematic diagram of sodium-ion batteries.

of "interlayer intercalation-micropore filling." However, its first-cycle Coulombic efficiency is less than 85%, which usually needs to be improved through surface modification (e.g., coating with amorphous carbon). Electrolytes: Mainly adopt the $NaPF_6$/carbonate system, which has obvious defects. On the one hand, the solubility of $NaPF_6$ in carbonate solvents is only 60% of that of $LiPF_6$; on the other hand, the interface stability between this system and the electrode is poor, which affects the battery cycle life. At present, the energy density of sodium-ion batteries is approximately 120–160 Wh/kg, only half of that of lithium-ion batteries. To achieve wider applications, it is necessary to break through the two core bottlenecks of slow electrode kinetics and poor interface compatibility [5].

1.3.3 All-Solid-State Batteries

All-solid-state batteries replace traditional liquid electrolytes with solid electrolytes, which can not only completely solve the safety hazards caused by lithium dendrite growth but also eliminate the risk of electrolyte combustion and explosion. Their theoretical energy density can reach 600–800 Wh/kg, far exceeding the level of existing lithium-ion batteries [8, 9]. As shown in Figure 1.6, a schematic diagram of the all-solid-state battery structure (including the cathode, anode, solid-state electrolyte, and MIEC/HEO material composition) is depicted. It presents the structure: solid electrolytes replace liquid ones (solving Li dendrite/flammability issues), with MIEC/HEO optimizing electrode-electrolyte compatibility, enabling high energy density and safety.

At present, the industry has mainly formed three technical routes: Oxide system: Represented by LLZO ($Li_7La_3Zr_2O_{12}$), it has an ionic conductivity of 10^{-4}–10^{-3} S/cm at room temperature and excellent chemical stability. However, this type of material has high brittleness (with a fracture toughness of only 1−2 MPa · $m^{1/2}$) and is prone to poor interface contact with the electrode [9]. Sulfide system: Typified by LGPS

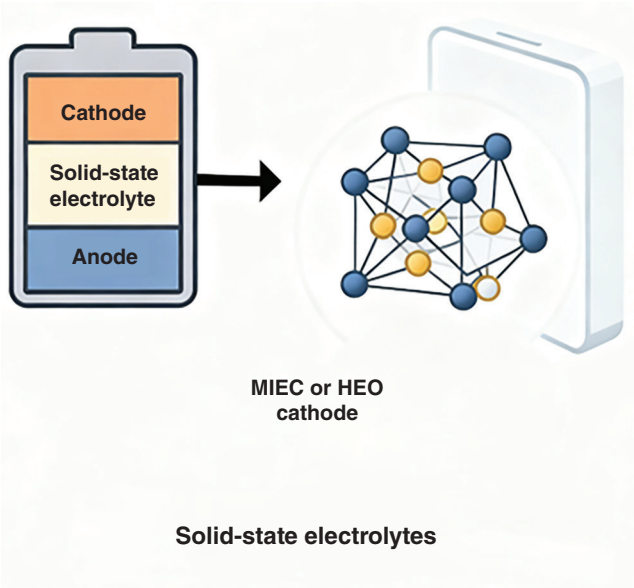


Figure 1.6 Schematic diagram of the all-solid-state battery structure.

($Li_{10}GeP_2S_{12}$), it has better room-temperature ionic conductivity (10^{-3}–10^{-2} S/cm) and good mechanical flexibility, which is convenient for processing and forming. However, it is prone to hydrolysis with moisture in the air (generating H_2S) and reacts violently with metallic lithium (generating Li_3P), so its stability needs to be improved [9]. Polymer system: Such as the PEO-LiTFSI system, which has the characteristics of bendability and stretchability and is suitable for flexible battery scenarios. However, its low-temperature performance is poor—the ionic conductivity drops to less than 10^{-6} S/cm below 0 °C, and its oxidation stability is poor (decomposing at voltages above 4.0 V) [10]. Overall, the core bottlenecks of all-solid-state batteries are concentrated on three aspects: "high solid-solid interface impedance, severe interface reactions, and poor mechanical compatibility." To achieve technological breakthroughs, it is necessary to make simultaneous efforts and conduct collaborative optimization from two aspects: interface regulation and electrolyte design [8].

1.3.4 Other New Battery Systems

Lithium-sulfur batteries: Their theoretical energy density is as high as 2600 Wh/kg, which is achieved through the multielectron transfer reaction of "$S_8 \rightarrow Li_2S$." However, they have obvious shortcomings: sulfur itself has extremely low conductivity (only 10^{-30} S/cm), and polysulfide shuttling occurs during the discharge process, which directly leads to rapid capacity fading of the battery. Zinc-ion batteries: They use aqueous electrolytes, which are safe without combustion and explosion risks, and their cost is only one-third of that of lithium-ion batteries, making them

particularly suitable for scenarios such as low-speed electric vehicles and backup power supplies. However, they also have prominent problems: the cycle stability of cathode materials (e.g., MnO_2) is poor (cycle life less than 500 cycles), and zinc dendrites tend to grow on the surface of the zinc anode, affecting battery life and safety. Potassium-ion batteries: They stand out due to the advantage of potassium resources—the abundance of potassium in the Earth's crust is 2.09%, and it can be directly compatible with graphite anodes for potassium intercalation, without the need to develop new anode materials specifically. However, due to the large radius of K^+ (1.38 Å), the structure of the cathode material is prone to collapse during intercalation and deintercalation. At present, their energy density can only reach 80–120 Wh/kg, which is difficult to meet high-capacity requirements. These emerging battery systems have shown unique potential in specific application scenarios, but to achieve large-scale commercialization, they all need to break through the two core bottlenecks of insufficient intrinsic material performance and difficult interface regulation [11].

1.4 Research Trend and Core Bottlenecks of Key Battery Components

1.4.1 Electrode Materials

1.4.1.1 Cathode Materials

High-nickel ternary cathode materials of lithium-ion batteries (e.g., NCM811) face a series of performance degradation problems during deep deintercalation: Ni^{3+}/Ni^{4+} undergoes strong hybridization with O 2p orbitals, which triggers lattice oxygen release—especially at voltages above 4.5 V, the amount of O_2 evolution increases sharply; at the same time, the H1−3→O1 phase transition occurs, leading to a 5–7% shrinkage of the material's lattice c-axis. The internal stress of the particles accumulates continuously, eventually generating microcracks. Observations via FIB-SEM show that these cracks will penetrate the entire particle after 100 cycles. Although lithium-rich manganese-based cathodes (e.g., $xLi_2MnO_3 \cdot (1-x)$NCM) can achieve a high capacity of 250–300 mAh/g, the Jahn-Teller effect caused by Mn^{3+} will lead to significant battery voltage fading (dropping from the initial 4.2 V to approximately 3.8 V), which affects the actual user experience. The cathode materials of sodium-ion batteries also have their own shortcomings: due to the large radius of Na^+ (1.02 Å), the diffusion coefficient of layered oxide $NaNi_{0.3}Co_{0.3}Mn_{0.4}O_2$ in the lattice is only 10^{-11} cm^2/s, resulting in poor rate performance (the capacity at 1C rate is only 70% of that at 0.1C rate); polyanionic $Na_3V_2(PO_4)_3$ has poor conductivity (only 10^{-6} S/cm), and carbon coating treatment is usually required to improve electron transport efficiency. At present, research hotspots in related fields focus on targeted performance optimization. For example, designing a "core-shell-gradient" structure for high-nickel cathodes—using high Ni content in the core to ensure capacity and high Mn/Al content in the outer layer to improve structural

stability; adopting Ti/Mg doping for high-lithium cathodes to inhibit Mn migration and alleviate voltage fading. However, most of these studies are limited to macro-performance improvement, and there is a lack of clear and in-depth understanding of atomic-level details such as the specific occupancy of doping elements in the lattice and the lattice matching degree between the coating layer and the matrix material [7].

1.4.1.2 Anode Materials

Although silicon-based anodes of lithium-ion batteries have outstanding theoretical capacity, they undergo a volume expansion of up to 300% during lithium intercalation. This severe volume change will lead to the pulverization of anode particles and repeated rupture and regeneration of the surface SEI layer, eventually resulting in a capacity retention rate of less than 50% after 50 cycles. Lithium metal anodes also face tricky problems: lithium dendrites tend to grow in liquid electrolytes (in-situ optical microscopy observations show that the length of these dendrites can reach 5–10 μm), and stripping pores appear in solid-state batteries (in-situ transmission electron microscopy (TEM) detection shows that the volume ratio of these pores exceeds 20%), which seriously affects battery safety and cycle stability. Hard carbon, a commonly used anode material for sodium-ion batteries, has a sodium storage capacity of 300–350 mAh/g, but its first-cycle Coulombic efficiency is less than 85%. Moreover, there are two controversial views in the industry regarding its sodium storage mechanism: "intercalation-adsorption" and "filling-adsorption," and no unified understanding has been formed yet. Current research hotspots in related fields focus on targeted modification and optimization. For example, nanostructuring (e.g., Si nanowires) or compounding with carbon materials (e.g., Si/graphene composite systems) is used for silicon-based anodes; and artificial SEI layers (e.g., Li_3N, LiF) are constructed for lithium metal anodes to improve performance. However, most of these studies focus on macro-effect improvement, and there is a lack of in-depth and systematic understanding of the dynamic correlation between "volume expansion—interface evolution—electrochemical performance" [12].

1.4.2 Electrolyte

1.4.2.1 Liquid Electrolyte

The $LiPF_6$/carbonate electrolyte system commonly used in lithium-ion batteries (mostly a mixed system of EC, EMC, and DMC) will undergo obvious oxidative decomposition when the charging voltage exceeds 4.5 V: the C-O bond in EC molecules is prone to cleavage (density functional theory (DFT) calculations show that its oxidation barrier is only 2.8 eV), thereby generating by-products such as CO_2 and Li_2CO_3. DEMS detection shows that the CO_2 gas production rate increases by 10 times at voltages above 4.5 V. At the same time, $LiPF_6$ in the electrolyte is prone to hydrolysis to generate HF—when the water content in the system exceeds 50 ppm, the HF concentration will exceed 10 ppm, which corrodes the cathode material and current collector. The electrolytes of sodium-ion batteries face another

type of problem: the solubility of commonly used $NaPF_6$ in carbonate solvents is only 60% of that of $LiPF_6$, and there is a strong solvation interaction between Na^+ and solvent molecules (the solvation energy is 15–20 kJ/mol higher than that of Li^+), which significantly increases the desolvation barrier of Na^+ and affects ion transport efficiency. At present, research hotspots in related fields focus on fluorinated electrolytes (e.g., fluorinated EC) and flame-retardant electrolytes (added with flame retardants such as triethyl phosphate). However, these solutions also have obvious shortcomings: the cost of fluorinated solvents is three to five times that of traditional solvents, and the addition of flame retardants will reduce the ionic conductivity of the electrolyte from approximately 10^{-2} S/cm to 5×10^{-3} S/cm [13].

1.4.2.2 Solid Electrolyte

Among the oxide electrolytes commonly used in solid-state batteries, LLZO ($Li_7La_3Zr_2O_{12}$) has an ionic conductivity of 10^{-4}–10^{-3} S/cm at room temperature, but it needs to be sintered at a high temperature above 1000 °C for forming. During this process, Li element volatilization is prone to occur, which further leads to an interface porosity of over 15% between the electrolyte and the electrode, affecting the interface contact effect. LGPS ($Li_{10}GeP_2S_{12}$) in sulfide electrolytes has more outstanding performance, with a room-temperature ionic conductivity of up to 10^{-3}–10^{-2} S/cm. However, it has obvious stability defects: it not only easily undergoes hydrolysis with moisture in the air but also reacts violently with metallic lithium to generate Li_3P, leading to a sharp increase in interface impedance to over 1000 $\Omega \cdot cm^2$. Polymer electrolytes such as the PEO-LiTFSI system have the advantages of good mechanical properties and bendability, which can be adapted to flexible battery scenarios. However, their low-temperature performance is extremely poor—the ionic conductivity drops to less than 10^{-6} S/cm below 0 °C, which is difficult to meet low-temperature application requirements. At present, research hotspots in the field of solid electrolytes focus on composite electrolytes, such as the LLZO-PEO composite system and the LGPS-carbon nanotube composite system. However, there are still cognitive blind spots in these composite systems: there is no clear understanding of the specific ion transport paths in them, the products generated after interface reactions, and their dynamic evolution processes [14].

1.4.3 Interface

1. Solid-Liquid Interface of Liquid Batteries (SEI/Cathode Electrolyte Interphase (CEI) Layers)
   At the solid-liquid interface of liquid lithium-ion batteries, an ideal SEI layer needs to meet the core requirements of "thickness less than 10 nm, dense structure, and high lithium-ion conductivity." However, the silicon-based anode undergoes a volume expansion of up to 300% during lithium intercalation. This severe expansion will lead to repeated rupture and regeneration of the surface SEI layer, which not only causes the electrolyte consumption to exceed 50% of the initial total amount but also significantly deteriorates

the battery cycle performance. On the cathode side, the CEI layer is affected by oxygen free radicals (e.g., O_2^-) released by the cathode. X-ray photoelectron spectroscopy (XPS) detection shows that the proportion of organic phase in the CEI layer increases from the initial 40% to approximately 70%. An excessively high proportion of organic phase will lead to a sharp increase in interface impedance, which impairs the kinetic performance of the battery. At present, there are still obvious cognitive gaps in the research on SEI and CEI layers: key issues such as the formation order of each component of the two layers and whether a self-healing mechanism exists during cycling have not been clarified. At the same time, there is a lack of effective methods to quantify the specific role of inorganic phases such as LiF in the interface layer.

2. Solid-Solid Interface of Solid-State Batteries
   In the solid-solid interface problem of all-solid-state batteries, high contact impedance is the primary challenge—in-situ atomic force microscopy (AFM) observations show that the actual contact area between metallic lithium and solid electrolyte is less than 30%, which makes the interface impedance account for over 60% of the total battery impedance and seriously affects ion transport efficiency. At the same time, interface reactions will exacerbate performance degradation: the reaction between metallic lithium and sulfide electrolyte LGPS generates Li_3P (the calculated reaction barrier is only 0.8 eV), and the contact between metallic lithium and oxide electrolyte LLZO generates $LiAlO_2$. TEM observations show that the thickness of such interface reaction layers is between 5 and 10 nm. In addition, the impact of mechanical incompatibility cannot be ignored. Metallic lithium undergoes volume changes during deposition and stripping, which leads to interface separation. The volume ratio of the formed pores can exceed 20%, further worsening the interface contact. At present, there are still obvious cognitive gaps in the research on the interface of solid-state batteries: the complete process from nucleation to growth of interface pores has not been clarified, and the coupling mechanism between electrochemical processes and mechanical effects has not been fully understood. These factors restrict the performance breakthrough of all-solid-state batteries [14, 15].

1.5 Evolution of Characterization Technology

As shown in Figure 1.7, a schematic diagram of the correlation between advanced characterization technologies and theoretical calculation methods (including in-situ characterization technologies, X-ray related technologies, and theoretical calculation methods such as DFT and molecular dynamics) is depicted. It links in-situ characterization (e.g., in-situ x-ray diffraction (XRD)/XPS) with DFT/MD, overcoming static offline method limits to enable multiscale analysis of battery material failure mechanisms.

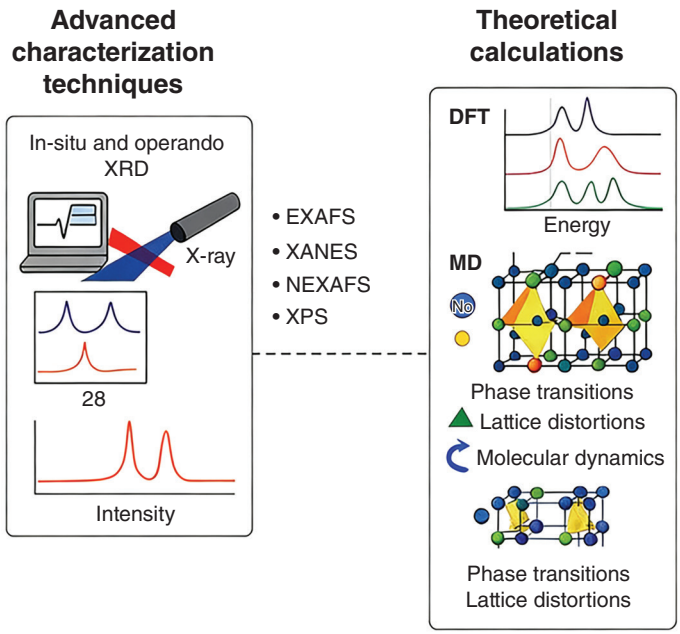


Figure 1.7 Schematic diagram of the correlation between advanced characterization technologies and theoretical calculation methods.

1.5.1 Limitations of Traditional Offline Characterization

Traditional offline characterization methods, such as ex-situ XRD, TEM, and XPS, can only capture "instant snapshots" of the battery in a static state. Specifically, ex-situ XRD can only compare the phase transition differences before and after battery cycling, and cannot track the onset voltage and evolution rate of phase transitions such as H1−3→O1. Ex-situ TEM cannot observe the complete real-time growth process of lithium dendrites, and can only infer their formation mechanism based on the morphology after cycling. Ex-situ XPS is also unable to clarify the formation order of each component of the SEI and CEI layers, and ultimately it is difficult to establish a direct correlation between "structure-performance-failure." For example, it cannot clearly explain the dynamic correlation between the capacity fading of silicon-based anodes and the rupture of the SEI layer.

1.5.2 Technical Requirements for Advanced Characterization

With the continuous development of battery materials toward high capacity, high voltage, and compounding, as shown in Figure 1.8, the industry has put forward three clear requirements for characterization technology: Spatial resolution: It needs to be further upgraded from the micron level (capable of observing particle morphology) to the atomic level (capable of identifying the occupancy of doping elements and the composition of interface phases). Temporal resolution: It needs

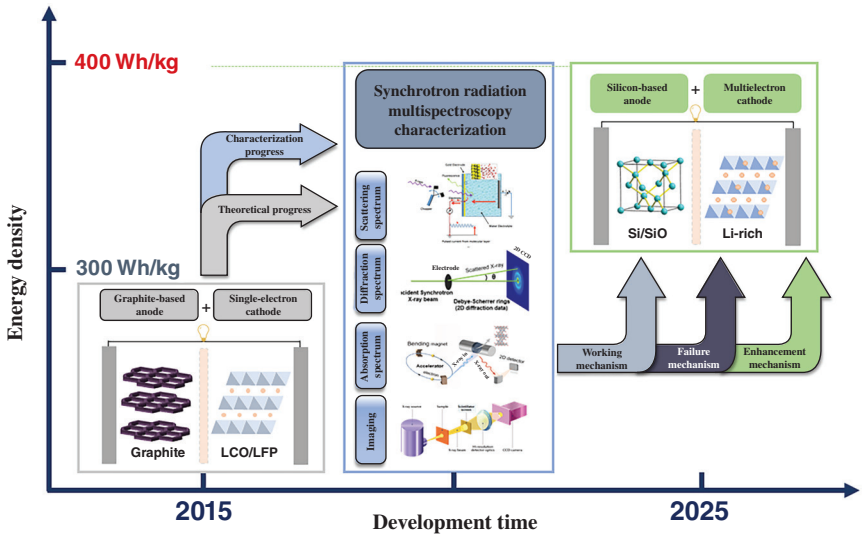


Figure 1.8 The urgent demand of the industry for advanced characterization technologies.

to be accelerated from the minute level (corresponding to charge-discharge curves) to the millisecond level (capable of capturing ion diffusion and interface reactions). Dimensional integrity: It needs to break through the limitation of single structural characterization (e.g., XRD) and realize multidimensional coupling analysis of structure, composition, electrochemistry, and mechanics [16].

1.5.3 Core Value of Advanced Characterization

Advanced characterization technology realizes the comprehensive analysis of the dynamic behavior of battery materials through in-situ testing modes and multitechnology coupling [17]. For example: In terms of dynamic structure tracking: In-situ synchrotron radiation XRD (with a spatial resolution of less than 1 μm and a temporal resolution of less than 10 s) can accurately capture the phase transition process of the cathode; in-situ aberration-corrected TEM (with atomic-level resolution) can clearly observe the microscopic arrangement of lithium deposition. In terms of composition and interface analysis: in-situ XPS (with a detection depth of less than 1 nm) can track the formation law of LiF in the CEI layer in real time; in-situ TOF-SIMS (with a spatial resolution of less than 10 nm) can reconstruct the elemental gradient distribution of the SEI layer. In terms of electrochemical-mechanical coupling characterization: in-situ AFM (with a mechanical resolution of less than 1 nN) can quantify the volume change of electrode particles; in-situ tensile testing combined with voltage measurement can establish the correlation between Co-O bond vibration and Co valence state. In terms of material design guidance, these in-situ characterization technologies can optimize the coating thickness of the cathode (to ensure that the proportion of LiF in the CEI layer exceeds 50%) and the volume expansion rate of the silicon-based anode (to control it within 150%), and ultimately build a complete research closed loop of "characterization-mechanism-design."

References

1 H. Du, H. Zhang, Climate neutrality in the EU and China: An analysis of the stringency of targets and the adaptiveness of the relevant legal frameworks, Review of European, Comparative & International Environmental Law 31(3) (2022) 495–509. https://doi.org/10.1111/reel.12453.

2 N. Azizi, H. Moradi, K. Rouzbehi, F. Mohammadi, HVDC grids stability enhancement through the integration of battery energy storage systems, IET Renewable Power Generation 18(15) (2024) 2838–2853. https://doi.org/10.1049/rpg2.12788.

3 X. Hu, Z. Wang, H. Zhang, Y. Song, J. Cui, J. Guo, M. Cao, Z. Wang, Y. Yao, Y. Huang, High-entropy design in battery materials for high performance electrochemical energy storage, Interdisciplinary Materials 4(6) (2025) 795–811. https://doi.org/10.1002/idm2.70013.

4 T.-H. Kim, J.-S. Park, S.K. Chang, S. Choi, J.H. Ryu, H.-K. Song, The current move of lithium ion batteries towards the next phase, Advanced Energy Materials 2(7) (2012) 860–872. https://doi.org/10.1002/aenm.201200028.

5 C. Li, L. Du, J. Ju, J. Niu, G. Xu, J. Zhao, G. Cui, Assessment of safety concerns in sodium-ion batteries, Advanced Energy Materials 15(40) (2025) e03209. https://doi.org/10.1002/aenm.202503209.

6 K. Kubota, M. Dahbi, T. Hosaka, S. Kumakura, S. Komaba, Towards K-ion and Na-ion batteries as "beyond Li-ion," The Chemical Record 18(4) (2018) 459–479. https://doi.org/10.1002/tcr.201700057.

7 L. Chang, A. Wei, S. Luo, S. Cao, X. Bi, W. Yang, R. Yang, J. Liu, Lithium-ion battery: A comprehensive research progress of high nickel ternary cathode material, International Journal of Energy Research 46(15) (2022) 23145–23172. https://doi.org/10.1002/er.8618.

8 S. Chai, Q. He, J. Zhou, Z. Chang, A. Pan, H. Zhou, Solid-state electrolytes and electrode/electrolyte interfaces in rechargeable batteries, ChemSusChem 17(3) (2024) e202301268. https://doi.org/10.1002/cssc.202301268.

9 K.J. Kim, M. Balaish, M. Wadaguchi, L. Kong, J.L.M. Rupp, Solid-state Li–metal batteries: Challenges and horizons of oxide and sulfide solid electrolytes and their interfaces, Advanced Energy Materials 11(1) (2021) 2002689. https://doi.org/10.1002/aenm.202002689.

10 J. Hou, J. Zhang, S. Wu, X. Liu, Y. Li, Z. Yan, K. Zhang, Y. Lu, J. Chen, Advanced design and characterization of polyether-based solid-state electrolytes for high-energy-density lithium batteries, Advanced Materials n/a(n/a) (2025) e15430. https://doi.org/10.1002/adma.202515430.

11 S. Kaskel, Lithium–Sulfur Batteries, Energy Technology 7(12) (2019) 1900940. https://doi.org/10.1002/ente.201900940.

12 M. Ezzedine, F. Jardali, I. Florea, M.-R. Zamfir, C.-S. Cojocaru, Nanostructuring strategies for silicon-based anodes in lithium-ion batteries: Tuning areal silicon loading, SEI formation/irreversible capacity loss, rate capability retention and electrode durability, Batteries & Supercaps 6(3) (2023) e202200451. https://doi.org/10.1002/batt.202200451.

13 W. Teng, J. Wu, Q. Liang, J. Deng, Y. Xu, Q. Liu, B. Wang, T. Ma, D. Nan, J. Liu, B. Li, Q. Weng, X. Yu, Designing advanced liquid electrolytes for alkali metal batteries: Principles, progress, and perspectives, Energy & Environmental Materials 6(2) (2023) e12355. https://doi.org/10.1002/eem2.12355.

14 Q. Zhou, X. Xiong, J. Peng, W. Wu, W. Fan, H. Yang, T. Wang, Y. Ma, F. Wang, Y. Wu, Tailored engineering on the interface between lithium metal anode and solid-state electrolytes, Energy & Environmental Materials 8(1) (2025) e12831. https://doi.org/10.1002/eem2.12831.

15 S.A. Pervez, G. Kim, B.P. Vinayan, M.A. Cambaz, M. Kuenzel, M. Hekmatfar, M. Fichtner, S. Passerini, Overcoming the interfacial limitations imposed by the solid–solid interface in solid-state batteries using ionic liquid-based interlayers, Small 16(14) (2020) 2000279. https://doi.org/10.1002/smll.202000279.

16 J. Wu, F. Ma, X. Liu, X. Fan, L. Shen, Z. Wu, X. Ding, X. Han, Y. Deng, W. Hu, C. Zhong, Recent progress in advanced characterization methods for silicon-based lithium-ion batteries, Small Methods 3(10) (2019) 1900158. https://doi.org/10.1002/smtd.201900158.

17 Z. Deng, X. Lin, Z. Huang, J. Meng, Y. Zhong, G. Ma, Y. Zhou, Y. Shen, H. Ding, Y. Huang, Recent progress on advanced imaging techniques for lithium-ion batteries, Advanced Energy Materials 11(2) (2021) 2000806. https://doi.org/10.1002/aenm.202000806.